# Entanglement Storage Units

Tommaso Caneva[1], Tommaso Calarco[1], and Simone Montangero[1]
[1]*Institut für Quanteninformationsverarbeitung, Universität Ulm, D-89069 Ulm, Germany*

(Dated: August 17, 2011)

We introduce a protocol to drive many body quantum systems into long-lived entangled states, protected from decoherence by big energy gaps. With this approach it is possible to implement scalable entanglement-storage units. We test the protocol in the Lipkin-Meshkov-Glick model, a prototype many-body quantum system that describes different experimental setups.

PACS numbers:

Entanglement represents the manifestation of correlations without a classical counterpart and it is regarded as the necessary ingredient at the basis of the power of quantum information processing. Indeed quantum information applications as teleportation, quantum criptography or quantum computers rely on entanglement as a crucial resource [1]. Within the current state-of-art, promising candidates for truly scalable quantum information processors are considered architectures that interface hardware components playing different roles like for example solid-state systems as stationary qubits combined in hybrid architectures with optical devices [3]. In this scenario, the stationary qubits are a collection of engineered qubits with desired properties, as decoupled as possible from one another to prevent errors. However, this architecture is somehow unfavorable to the creation and the conservation of entanglement. Indeed, it would be desirable to have a hardware where "naturally" entanglement is present and that can be prepared in a highly entangled state that persists without any external control: the closest quantum entanglement analogue of a classical information memory support, i.e. an *entanglement-storage unit* (ESU). Such hardware once prepared can be used at later times (alone or with duplicates) – once the desired kind of entanglement has been distilled – to perform quantum information protocols [1].

The biggest challenge in the development of an ESU is entanglement frailty: it is strongly affected by the detrimental presence of decoherence [1]. Furthermore the search for a proper system to build an ESU is undermined by the increasing complexity of quantum systems with a growing number of components, which makes entanglement more frail, more difficult to characterize, to create and to control [2]. Moreover, given a many body quantum system, the search for a state with the desired properties might be very difficult. Indeed, a direct and comprehensive study of a many body quantum system is an exponentially hard task in the system size. Nevertheless, in many-body quantum systems entanglement naturally arises: for example –when undergoing a quantum phase transition – in proximity of a critical point the amount of entanglement possessed by the ground state scales with the size [2, 4]. Unfortunately, due to the closure of the energy gap at the critical point, the ground state is an extremely frail state: even very little perturbations might destroy it, inducing excitations towards other states. Very recently, the entanglement properties of the eigenstates of many-body Hamiltonians have been investigated, and it has been shown that in some cases they are characterized by entanglement growing with the system size [5, 13].

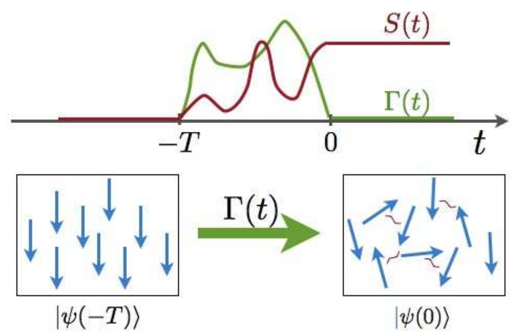


FIG. 1: (Color online) Entanglement Storage Units protocol: a system is initially in a reference state $|\psi(-T)\rangle$, e.g. the ground state, and is optimally driven via a control field $\Gamma(t)$ in an entangled eigenstate $|\psi(0)\rangle$, protected from decoherence by an energy gap.

In this letter we show that by means of recently developed optimal control technique [7] it is possible to identify and prepare a many body quantum system in robust, long-lived entangled states (ESU states). More importantly, we drive the system towards ESU states without the need of any apriori information on the system, either about the eigenstates or about the energy spectrum. Finally, we show that properly prepared systems can be effectively used as ESU exploiting the fact that ESU states are well protected by large energy gaps.

Recently, optimal control has been used to drive quantum systems in entangled states or to improve the generation of entanglement [6]. However, here we have in mind a different scenario: to exploit the control to steer a system into a highly entangled state that is stable and robust even after switching off the control (see Fig. 1). In the following we show that ESU states are gap-protected entangled eigenstates of the system Hamiltonian *in the absence* of the control. Here we show that for an experimentally relevant model this is indeed possible, and that it is possible to drive the system in gap-protected states. We show that the ESU states, although not being characterized by the maximal entanglement sustainable by the system, are characterized by entanglement that grows with the system size. Once a good ESU state has been detected, due to its robustness it can be stored, characterized, and thus used for later quantum information processing.

*Protocol* - As depicted in Fig. 1, we consider the general scenario of a system represented by a Hamiltonian $H_o$ with an additional tunable term $H_1[\Gamma]$, where $\Gamma(t)$ is the driving field, starting in an initial state $|\psi_0\rangle$, not necessarily entangled, in which the system can be easily prepared. The Hamiltonian is then $H = H_0 + H_1[\Gamma]$, where the control parameter is initially set at a constant value (in particular it can vanish, $\Gamma(0) = 0$). The control field is modulated $\Gamma(t)$ for $-T < t < 0$ with the condition that at time $t = 0$ the control field is $\Gamma(-T) = \Gamma(0)$ (absence of control). A CRAB optimization is then performed –in the time interval $[-T, 0]$– with the goal of minimizing the cost function $\mathcal{F}$ (see [7] for details of the method):

$$\mathcal{F}(\lambda)_{|\psi(T)\rangle} = -S + \lambda \frac{\Delta E_0}{E_0}, \tag{1}$$

where $S$ represents a measure of entanglement, $\Delta E_0 = \sqrt{\langle\psi|H_0^2 - \langle H_0\rangle^2|\psi\rangle}$ and $E_0 = \langle\psi|H_0|\psi\rangle$ correspond respectively to the energy fluctuations and the energy computed with respect to $H[\Gamma_0]$, $\lambda$ is a Lagrange multiplier, and the cost function is evaluated on the optimized evolved state $|\psi(0)\rangle$. As shown in the following, the inclusion in $\mathcal{F}$ of the constraint on the energy fluctuations is the crucial ingredient to stabilize the result of the optimization and possibly to steer the system into an ESU state.

*Model* - Here we provide an important example of this approach, based on the the Lipkin-Meshkov-Glick (LMG) model [8]; we prepare an ESU maximizing the Von Neumann entropy of a bipartition of the system and we model the action of the surrounding environment with noise terms in the Hamiltonian. However, our protocol is compatible with different entanglement measures and different models, and with a straightforward generalization it can adapted to a full description of open quantum systems [15]. The LMG model represents a prototype of the challenge we address: it describes different experimental setups [3, 10], and the entanglement properties of the eigenstates are in general not known. Indeed, the entanglement properties of the eigenstates of one-dimensional many-body quantum systems have been related with the corresponding conformal field theories [5]; however for the LMG model, to our knowledge, this study has never been performed and a conformal theory is not available [9]. Finally, the optimal control problem we address is highly non-trivial as the control field is global and space-independent with no single-site addressability [6].

The LMG Hamiltonian describes an ensemble of spins with infinite-range interaction and is written as:

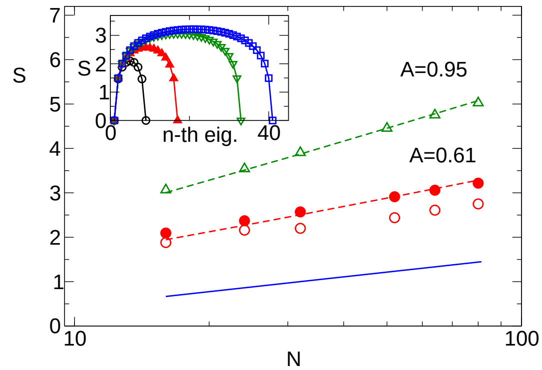


FIG. 2: (Color online) LMG model: Ground state entanglement at the critical point of the (blue full line); central eigenstate entanglement at $\Gamma = 10$ (full red circles); maximal eigenstate entanglement obtained with the optimization for $\lambda \neq 0$ (empty red circles) and $\lambda = 0$ (green triangle). The red (green) dashed line is numerical fit $A \cdot \log_2(N/2+1)$ with $A = 0.61$ ($A = 0.95$). Inset: Static entanglement $S$ of the eigenstates at $\Gamma = 10$ for different system sizes $N = 16, 32, 64, 80$. The eigenstates are ordered according to their energy, i.e. $n = 1$ corresponds to the ground state.

$H^{\mathrm{LMG}} = -\sum_{i<j}^{N} J_{ij}\sigma_i^x\sigma_j^x - \Gamma(t)\sum_i^N \sigma_i^z$ , where $N$ is the total number of spins, $\sigma_i^\alpha$'s ($\alpha = x, y, z$ ) are the Pauli matrices on the $i$th site and $J_{ij} = J/N$ (infinite range interaction). By introducing the total spin operator $\vec{J} = \sum_i \vec{\sigma}_i$, the Hamiltonian can be rewritten, apart from an additive constant, as

$$H = -\frac{1}{N} J_x^2 - \Gamma J_z, \tag{2}$$

(from now on we set $J = 1$ and $\hbar = 1$). The Hamiltonian hence commutes with $J^2$ and does not couple states having a different parity of the number of spins pointing in the magnetic field direction: $[H, J^2] = 0$ and $[H, \prod_i \sigma_i^z] = 0$. The symmetries of the Hamiltonian imply that the dynamics is restricted to subspaces of fixed total magnetization $J$; a convenient basis for such subspaces is represented by the Dicke states $|J, J_z\rangle$ with $-J < J_z < J$ [11]. In the thermodynamical limit the system undergoes a 2nd order QPT from a quantum paramagnet to a quantum ferromagnet at a critical value of the transverse field $|\Gamma_c| = 1$. There is no restriction to the initial value of $\Gamma_0$ (in the implementation of Ref. [3] it goes to infinity when the control lasers are switched off) and to the initial state $|\psi_0\rangle$: we choose $\Gamma_0 \gg 1$, corresponding to the paramagnetic phase and as initial state $|\psi_0\rangle$, the ground state of $H[\Gamma_0]$, i.e. the separable state in which all the spins are polarized along the positive $z$-axis. A convenient measure of the entanglement in the LMG model is given by the von Neumann entropy $S_{L,N} = -\mathrm{Tr}(\rho_{L,N}\log_2 \rho_{L,N})$ associated to the reduced density matrix $\rho_{L,N}$ of a block of $L$ spins out of the total number $N$, which gives a measure of the entanglement present between two bipartitions of a quantum system [12]. In our analysis we consider two equal bipar-

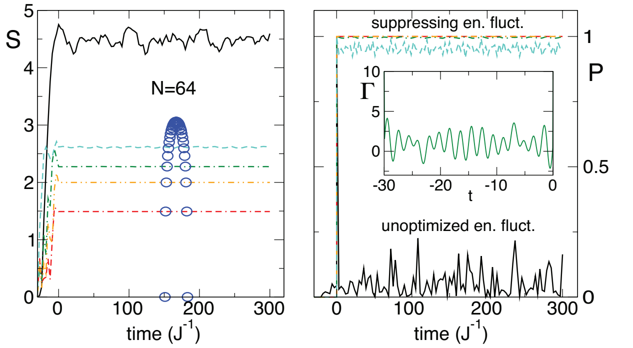


FIG. 3: (Color online) Entanglement entropy $S(t)$ (left) and survival probability $P(t)$ (right) as a function of time for different $\lambda$ values: $\lambda = 0$ (black) continuous, $\lambda = 5$ (red) dash-dash-dotted, $\lambda = 1.8$ (green) dot-dashed, $\lambda = 1.9$ (orange) dot-dot-dashed, $\lambda = 1.2$ (cyan) dashed line. Blue circles represent the entropy of the eigenstates for $N = 64$ and $\Gamma_0 = 10$. Inset: Optimal driving field $\Gamma(t)$ for $\lambda = 1.8$ and $N = 64$ (time unit $J^{-1}$).

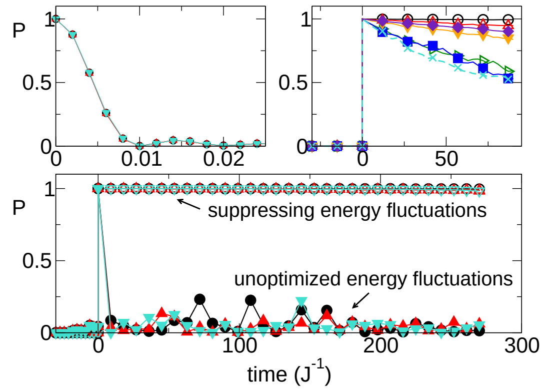


FIG. 4: (Color online) Lower panel: Survival probability $P(t)$ as a function of time in the presence for three realizations of the noise with $I_\alpha = I_\beta = 0.01$ at frequency $\nu_R$, system size $N = 64$, and $\lambda = 1.8$ (full symbols) or $\lambda = 0$ (empty symbols). Upper left panel: Blow up of the region around $t = 0$. Upper right panel: Survival probability $P(t)$ as a function of time, averaged over 30 noise instances for $I_\alpha = I_\beta = 0.2$, $N = 64$, $r = 1.8$, and different noise frequencies. The worst case is for $\nu_R = 0.78J$.

titions, i.e. $S \equiv S_{N/2,N}$. In the inset of Fig. 2 we report the entanglement $S_{N/2,N}$ of the eigenstates deeply inside the paramagnetic phase at $\Gamma = 10$, for systems of different sizes. Clearly, also far from the critical point $\Gamma = 1$ many eigenstates possess a remarkable amount of entanglement that scales with the system size. The effect is shown more clearly in Fig. 2, where the entanglement of the central eigenstate (red full circles) at $\Gamma_0 = 10$ is compared with the entanglement of the ground state at the critical point (blue continuous line, from Ref. [12]). Both sets of data show a logarithmic scaling with the size, but the entanglement of the central eigenstate is systematically higher and grows more rapidly.

*Dynamics.*— We prepare the system in the ground state of the Hamiltonian $H = H_0 + H_1(\Gamma_0)$ so that in the absence of control, i.e., $\Gamma \equiv \Gamma_0$ independent from the time, the state does not evolve apart from a phase factor. After the action of the CRAB-optimized driving field $\Gamma(t)$ for a time $T$ the state is prepared in $|\psi(0)\rangle$ (a typical optimal pulse is shown in the inset of Fig. 3), we observe the evolution of the state over times $t > 0$. The behavior of the entanglement is shown in the left panel of Fig. 3 for different values of the weighing factor $\lambda$ and $N = 64$; the control is active for negative times, i.e., in the interval $[-T, 0]$. For $\lambda = 0$ highly entangled states are produced, however the entanglement $S(t)$ oscillates indefinitely with the time, reflecting the fact that the system state is changing over time. On the contrary, if the energy fluctuations are included in the cost function ($\lambda \neq 0$), the optimal driving field steers the system into entangled eigenstates, as confirmed by the absence of the oscillations in the entanglement and by the entanglement eigenstate reference values (empty blue circles). These results are confirmed by the survival probability in the initial state $P(t) = |\langle\psi(0)|\psi(t)\rangle|^2$ reported in the right panel of Fig. 3: the state prepared with $\lambda = 0$ decays over very fast timescales $\tau_0$, while for $\lambda \neq 0$ it remains close to the unity for very long times $\tau_\lambda >> \tau_0$. The small residual oscillations for $N = 64$ and $\lambda = 1.2$ are due to the fact that in this case the optimization leads to a state corresponding to an eigenstate up to 98%. We repeated the optimal preparation for different system sizes and initial states, and show the entanglement of the optimized states for $\lambda = 0$ (empty green triangles) and $\lambda \neq 0$ ( $\Delta E_0/E_0 < 0.05$, $P > 95\%$ empty red circles) for different system sizes in Fig. 2. In all cases a logarithmic scaling with the size is achieved.

*Noise.*— A reliable ESU should be robust against external noise and decoherence even when the control is switched off, in such a way that it could be used for subsequent quantum operations. In order to test the robustness of the optimized states, we model the effect of decoherence by adding a random telegraph noise and we monitor the time evolution in such noisy environment [1]. In particular we study the evolution induced by the Hamiltonian

$$H = -\frac{1}{N}[1 + I_\alpha \alpha(t)]J_x^2 - \Gamma_0[1 + I_\beta \beta(t)]J_z \qquad (3)$$

where $\alpha(t), \beta(t)$ are random functions of the time with a flat distribution in $[-I_j, I_j]$ $(j = \alpha, \beta)$, changing random value every typical time $1/\nu$. The case $I_\alpha = I_\beta = 0$ corresponds to a noiseless evolution. The first important observation is that the frequency $\nu$ of the signal fluctuations is crucial in determining its effects [14]. Indeed in the right upper panel of Fig. 4, the survival probability $P(t)$ is plotted as a function of the time in the presence of a strong noise, $I_\alpha = I_\beta = 0.2$, for a system of $N = 64$ spins and for a given initial optimal state obtained with $\lambda = 1.8$ (corresponding to the third eigenstate in Fig. 3). When $\nu$ is either too low (empty circles) or too high

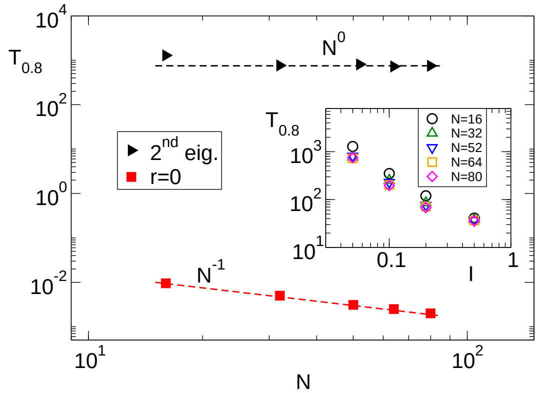


FIG. 5: (Color online) Time $T_{0.8}$ required to reduce the survival probability $P$ below 0.8 for different prepared states $|\psi(0)\rangle$ with $\lambda = 0$ (red squares) and $\lambda \neq 0$ (black triangles) as a function of the system size $N$. The dashed lines are fits of the four rightmost points (biggest system sizes) resulting in $N^{-0.97}$ and $N^{-0.03}$ respectively. Inset: Time $T_{0.8}$ as a function of the intensity $I = I_\alpha = I_\beta$ of the disorder for different system sizes $N$.

(full diamonds) the effect of the noise is reduced; however around a resonant frequency $\nu_R$ (dashed line with crosses) its effect is enhanced and the state is quickly destroyed. We checked that the resonant frequency is the same for different eigenvalues, different sizes, and different noise strengths (data not shown), reflecting the fact that in the paramagnetic phase ($\Gamma_0 \gg 1$) the gap separating the eigenstates is proportional to $\Gamma_0$ independently of the size of the system and of the state itself, see Eq. (2). Therefore we analyze this worst case scenario, setting $\nu = \nu_R$ from now on. The results of this analysis, show that ESU states – differently from the states produced optimizing only entanglement – are extremely robust to noise at the resonant frequency. This is shown in Fig. 4 where we compare the survival probability $P(t)$ for three instances of the disorder at the resonant frequency with an intensity of the disorder $I_\alpha = I_\beta = 0.01$. The noise-induce dynamics of the states obtained optimizing only with respect to the entanglement (i.e. setting $\lambda = 0$) drastically depends on the (in general unknown) details of the noise affecting the system, as shown by the different evolutions induced by different instances of the noise. Thus, such states cannot be used as ESU, unlike those prepared with $\lambda \neq 0$ that are stable, noise-independent long-living entanglement states. Finally, in Fig. 5 we study the decay times of the survival probability $P(t)$ studying the time $T_{0.8}$ needed to drop below a given threshold $P_{min} = 0.8$ as a function of the system size $N$ and of the intensity of the disorder $I = I_\alpha = I_\beta$ (inset). These results clearly show that $T_{0.8}$ for ESU states is almost independent from the system size, reflecting the fact that the energy gaps in this region of the spectrum are mostly size independent. Notice that, on the contrary, $T_{0.8}$ for maximally entangled states decays linearly with the system size and that there are more than four orders of magnitude of difference in the decay times $\tau_\lambda$ and $\tau_0$. Finally, the inset of Fig. 5 shows that the scaling of $T_{0.8}$ with the noise strength for ESU states is approximately linear and again depends very weakly on the system size $N$.

*Conclusions.*— Exploiting optimal control we proposed a method to steer a system into apriori unknown eigenstates satisfying desired properties. We demonstrated, on a particular system, that this protocol can be effectively used to build long-lived entangled states with many-body systems, indicating a possible implementations of an Entanglement Storage Unit scalable with the system size. The presented method is compatible with different measures of entanglement and it can be extended to any other property one is interested in, as for example the squeezing of the target state. It can be applied to different systems with apriori unknown properties: optimal control will select the states (if any) satisfying the desired property and robust to system perturbations. We underscore that an adiabatic strategy is absolutely ineffective for this purpose, as transitions between different eigenstates are forbidden. Applying this protocol to the full open-dynamics description of the system, e.g. via a CRAB optimization of the Lindblad dynamics as done in [16], will result in an optimal search of a Decoherence Free Subspace (DFS) with desired properties [17]. If no DFS exists, the optimization would lead the system in an eigenstate of the superoperator with longest lifetime and desired properties [15]. Although the state so prepared may be unstable over long times, it represents the best and most robust state attainable, and additional (weak) control might be used to preserve its stability. Finally, working with excited states would reduce finite temperature effects, relaxing low temperatures working-point conditions, simplifying the experimental requirements to build a reliable ESU.

We acknowledge discussions with M. D. Lukin, and support from the EU projects AQUTE, PICC, the SFB/TRR21 and the BWgrid for computational resources.


[1] M. Nielsen and I. L. Chuang, *Quantum Computation and Quantum Information* (Cambridge University Press, 2000).

[2] L. Amico, R. Fazio, A. Osterloh, and V. Vedral, Rev. Mod. Phys. **80**, 517 (2008). A. Osterloh, L. Amico, G. Falci, and R. Fazio, Nature **416**, 608 (2002).

[3] K. Baumann, C. Guerlin, F. Brennecke, and T. Esslinger, Nature **464**, 1301 (2010). K. Baumann, R. Mottl, F. Brennecke, and T. Esslinger (2011), arXiv:1105.0426.

[4] G. Vidal, J. Latorre, E. Rico, and A. Kitaev, Phys. Rev.

Lett. **90**, 227902 (2003).
[5] V. Alba, M. Fagotti, and P. Calabrese, J. Stat. Mech. p. P10020 (2009).
[6] F. Platzer, F. Mintert, and A. Buchleitner, Phys. Rev. Lett. **105**, 020501 (2010). X. Wang, A. Bayat, S. G. Schirmer, and S. Bose, Phys. Rev. A **81**, 032312 (2010).
[7] P. Doria, T. Calarco, and S. Montangero, Phys. Rev. Lett. **106**, 190501 (2011); T. Caneva, T. Calarco, and S. Montangero (2011), arXiv:1103.0855.
[8] H. J. Lipkin, N. Meshkov, and A. J. Glick, Nucl. Phys. **62**, 188 (1965).
[9] J. I. Latorre and A. Riera, J. Phys. A: Math. Theor. **42**, 504002 (2009).
[10] R. Bucker, J. Grond, S. Manz, T. Berrada, T. Betz, C. Koller, U. Hohenester, T. Schumm, A. Perrin, and J. Schmiedmayer, Nat. Phys. (2011).
[11] T. Caneva, R. Fazio, and G. E. Santoro, Phys. Rev. B **78**, 104426 (2008).
[12] J. I. Latorre, R. Orus, E. Rico, and J. Vidal, Phys. Rev. A **71**, 064101 (2005).
[13] F. C. Alcaraz, M. Berganza, and G. Sierra, Phys. Rev. Lett. **106**, 201601 (2011).
[14] P.Facchi, S.Montangero, R.Fazio, and S.Pascazio Phys. Rev. A **71**, 060306 (2005).
[15] T.Caneva, T.Calarco, S.Montangero, in preparation.
[16] F. Caruso, S. Montangero, T. Calarco, S. F. Huelga, and M. B. Plenio (2011), arXiv:1103.0929.
[17] G. M. Palma, K. A. Suominen, and A. K. Ekert, Proc. Roy. Soc. Lond. A **452**, 567 (1996); L.-M Duan and G.-C. Guo, Phys. Rev. Lett. **79**, 1953 (1997); P. Zanardi and M. Rasetti, Phys. Rev. Lett. **79**, 3306 (1997).